Journal of the American Heart Association

ORIGINAL RESEARCH

Renal Denervation Improves Uremic Cardiomyopathy in Rats With Chronic Kidney Disease

Philipp Markwirth, MD; Simina-Ramona Selejan, MD; Mathias Hohl, PhD; Stefan J. Schunk, MD; Andreas Müller, MD; Stefan Wagenpfeil, PhD; Lea Wagmann, PhD; Florian Kahles, MD; Mert Tokcan, MD; Markus Therre, MD; Emiel P. C. van der Vorst, PhD; Matthias Rau, MD; Heidi Noels, PhD; Julia Wollenhaupt, PhD; Felix Mahfoud, MD; Michael Böhm, MD

BACKGROUND: Chronic kidney disease (CKD) is an independent cardiovascular risk factor. Patients with CKD develop uremic cardiomyopathy characterized by activation of the sympathetic nervous system, left ventricular hypertrophy, and accumulation of uremic toxins such as indoxyl sulfate (IS). The aim of this study was to assess the effects of renal denervation (RDN) on uremic cardiomyopathy in a rat model of CKD.

METHODS: Sprague–Dawley rats were fed a standard chow (control group, n=6) or a 0.25% adenine-enriched chow (n=16) for 16 weeks to induce CKD. After 4 weeks, CKD rats with CKD were subjected to bilateral RDN (AD-RDN, n=8) or to sham operation (AD, n=8). Blood pressure measurements, echocardiography, and cardiac magnetic resonance imaging were deployed during the experiment. Left ventricular hypertrophy was evaluated histologically. IS was measured using ELISA. In H9C2 cardiomyoblasts, the hypertrophic effects of IS were characterized in vitro.

RESULTS: In AD rats, left ventricular septal wall thickness (2.37±0.036 versus 1.91±0.014 mm in CTRL, P <0.0001), E/A ratio, and cardiomyocyte size were significantly increased. Following RDN, left ventricular wall thickness (P <0.0001 versus AD), E/A ratio (P <0.0001 versus AD), and myocyte hypertrophy were significantly reduced. Plasma IS was increased in AD (0.79±0.07 versus 0.2±0.12 µg/mg in the control group, P=0.0044) and reduced in AD-RDN (P=0.0073 versus AD). Urinary IS remained unchanged after RDN, whereas hepatic concentration of IS decreased after RDN (P=0.023). Plasma IS correlated with left ventricular hypertrophy (r=0.779, P <0.0001). Stimulation of H9C2 cardiomyoblasts with IS or serum from AD rats showed an increase in cell size (P=0.0015), whereas AD-RDN serum showed no effect.

CONCLUSIONS: In a rat model of CKD, improved cardiac function following RDN was associated with reduced plasma concentrations of IS. To the present, IS remains a persistent clinical concern in patients with CKD due to its inefficient removal by conventional hemodialysis and its significant role in promoting both kidney and myocardial disease. Thus, RDN may ameliorate uremic cardiomyopathy by reducing IS and potentially represents a treatment option for patients with CKD and cardiovascular disease. Clinical trials are warranted to investigate the effects of RDN on cardiovascular outcomes in patients with CKD.

Key Words: chronic kidney disease ■ indoxyl sulfate ■ left ventricular hypertrophy ■ renal denervation ■ uremic cardiomyopathy

Chronic kidney disease (CKD) is a major risk factor for cardiovascular disease (CVD).[1] CVD is the leading cause of death in CKD and occurs more frequently than the progression to end-stage renal disease.[1] Both CVD and CKD share common risk factors such as hypertension, diabetes, or dyslipidemia, explaining some but not the total risk in CKD. Large epidemiological studies demonstrated an excess

Correspondence to: Philipp Markwirth, MD, Klinik für Innere Medizin III, IMED, Kirrbergerstraße 100, Universitätsklinikum des Saarlandes, 66421 Homburg/Saar, Germany. Email: philipp.markwirth@uks.eu

Supplemental Material is available at https://www.ahajournals.org/doi/suppl/10.1161/JAHA.124.038785

For Sources of Funding and Disclosures, see page 11.

JAHA is available at: www.ahajournals.org/journal/jaha

RESEARCH PERSPECTIVE

What Is New?

- In patients with chronic kidney disease, accumulation of the uremic toxin indoxyl sulfate is associated with left ventricular hypertrophy.
- Renal denervation was shown to reduce plasma indoxyl sulfate and mitigate left ventricular hypertrophy.

What Question Should Be Addressed Next?

- The precise mechanisms by which renal denervation influences indoxyl sulfate levels remain elusive, and further research is needed to explore this intriguing relationship.

Nonstandard Abbreviations and Acronyms

AD	adenine-fed sham-denervated group
AD-RDN	adenine-fed renal denervated group
CKD	chronic kidney disease
CTRL	control group
CVD	cardiovascular disease
LVH	left ventricular hypertrophy
RDN	renal denervation

cardiovascular morbidity and mortality in CKD, which cannot be fully explained by traditional risk factors.[2] Patients with CKD may develop a uremic cardiomyopathy, a condition characterized by left ventricular hypertrophy, fibrosis, diastolic dysfunction, and susceptibility for arrhythmias,[3] also known as Cardiorenal Syndrome Type IV or chronic renocardiac syndrome.[4] Emerging evidence suggests that uremic toxins play a major role in uremic cardiomyopathy.[3] The low-molecular and protein-bound uremic toxin indoxyl sulfate (IS) is of particular interest, because it has been shown to contribute to the progression of both CKD and CVD.[5] Both in vitro and in vivo studies found that IS promotes cardiac hypertrophy and inflammation and that inhibition of IS with an oral adsorbent can mitigate these effects.[6,7] Importantly, IS is highly bound to plasma proteins, preventing it from being eliminated by conventional hemodialysis. CKD associates with increased activity of the sympathetic nervous system.[8] In fact, this overactivity of the sympathetic nervous system is thought to contribute to cardiovascular mortality in CKD.[9] Renal denervation (RDN) reduces not only renal sympathetic tone, but also central sympathetic activity.[10] Furthermore, RDN was shown to reduce left ventricular (LV) hypertrophy partly independent of blood pressure (BP).[11] We investigated the influence of RDN on plasma concentrations of IS and tested the hypothesis that RDN ameliorates uremic cardiomyopathy in a rat model of CKD.

METHODS

The data that support the findings of this study are available from the corresponding author upon reasonable request.

Animal Model

The animal studies complied with the *Guide for the Care and Use of Laboratory Animals* (United States National Institutes of Health, 8th edition, revised 2011) and conform to the German law for the protection of animals. They were approved by the regional Animal Welfare Inspectorate (Saarländisches Landesamt für Verbraucherschutz, #35/2017). Animal studies were reported in compliance with the Animal Research: Reporting of In Vivo Experiments guidelines.

Male Sprague–Dawley rats (n=22, 6 weeks of age) were obtained from Charles River (Germany) and kept under standard conditions (12 hours dark/light cycle). Rats had free access to a standard chow and drinking water ad libitum. CKD was induced in 16 rats by feeding a 0.25% (w/w) adenine-containing diet, while 6 rats served as controls (CTRL, n=6). After 4 weeks, rats receiving the adenine-enriched diet were randomly assigned to either bilateral RDN (AD-RDN, n=8) or sham-surgery (AD, n=8). CTRL were also subjected to sham-surgery. After a total of 16 weeks, all rats were euthanized under deep anesthesia and analgesia (intraperitoneal ketamine 80 mg/kg body weight, xylazine 6 mg/kg body weight, and 2.5% isoflurane) and organs were harvested for further analyses.

Metabolic Cages and Blood Sampling

At week 4 and at week 15, rats were placed in metabolic cages to collect urine samples. Blood samples were obtained during the experiment from the tail vein and shortly before euthanized by cardiac puncture. A chemistry analyzer (AU480, Beckman Coulter, Krefeld, Germany) was used to measure plasma and urinary concentration of creatinine and urea.

BP Measurement

Systolic and diastolic BP were measured by either a catheter-based telemetry system (HD-S11-F0, Data Sciences International, St. Paul, MN) (CTRL: n=2; AD: n=3; AD-RDN: n=3) or plethysmographically using

a tail-cuff device (Visitech Systems with BP-2000 Analysis Software) twice weekly (CTRL: n=4, AD: n=5; AD-RDN: n=5). The telemetry system was implanted into the abdominal aorta as described previously 2 weeks before the start of the experiment.[12] In rats undergoing cardiac magnetic resonance imaging (MRI), BP was measured plethysmographically using a tail-cuff device. At the end of the experiment, rats were placed in a cage and 3 consecutive measurements were performed after 30 minutes of resting. Data are presented as the mean±SEM.

Renal Denervation

Bilateral RDN was performed after 4 weeks of adenine feeding in the respective groups as described previously.[13] Rats were placed in a supine position and anesthesia was achieved by 1.5% to 2.5% isoflurane. Both kidneys were surgically denervated by stripping the adventitia from the renal artery. Thereafter, a 20% phenol/ethanol solution was applied circumferentially to moisten the renal artery for 5 minutes to chemically destroy remaining nerve fibers. In sham-operated animals, the kidneys were exposed without performing RDN.

Echocardiography

Echocardiography was performed in all animals at baseline, at 4 weeks, and shortly before euthanasia at week 15 (GE Healthcare LOGIQ S6 with 12-MHz transducer). Rats were anesthetized with 1% isoflurane. Left ventricular end-systolic diameter, left ventricular end-diastolic diameter as well as LV wall thickness were measured by M-mode in the parasternal long-axis and short-axis view. In order to assess diastolic function, a pulsed-wave Doppler sample was placed in between the mitral valve leaflet tips in the apical 4-chamber view to obtain transmitral diastolic peak early (E) and atrial (A) velocities to yield E/A ratio.

Cardiac MRI

Cardiac MRI was performed using a 9.4-T animal scanner (Biospec Avance III 94/20, Bruker BioSpin, Germany) with rats under general anesthesia (1.5% isoflurane). Body temperature, ventilation, and ECG were continuously monitored. Cine FLASH sequences were obtained in 2-chamber view (TR 18 milliseconds, TE 1.8 milliseconds, field of view 25.6×25.6 mm, slice thickness 1 mm, interslice gap 0.5 mm). To assess cardiac function, 6 to 8 sequences in the 2-chamber view were created. Image analysis was done using the freely available software Segment v2.0 R4265 (Medviso, segment.heiberg.se) medical image analysis software. Left ventricular hypertrophy was determined by measuring LV wall thickness in the anterior, septal, and inferior wall in all 2-chamber view sequences, and means were calculated by the image analysis software. Also, end-systolic, end-diastolic volumes, and peak filling rate were determined after segmentation of all 2-chamber view images.

Hematoxylin–Eosin Staining

Immediately after euthanasia, hearts were fixed in buffered 4% formaldehyde for 48 hours and imbedded in paraffin. A microtome was used to cut 3-µm sections that were fixed at 56 °C overnight. Sections were then deparaffinized, rehydrated, and stained with hematoxylin and eosin (HE, Morphisto, Frankfurt a. M., Germany). Images were acquired using a whole slide scanner (Aperio Versa 8, Leica Biosystems, Wetzlar, Germany) and analyzed using the corresponding Aperio ImageScope software. To determine myocyte hypertrophy, the cross-sectional area of LV cardiomyocytes was measured in cells that were orthogonally cut (round in shape, nucleus centered) and an average was calculated.

Immunostaining for Tyrosine Hydroxylase

For immunofluorescence-staining of LV tyrosine hydroxylase, sections were deparaffinized and hydrated as described above. After incubating in 0.05% citraconic anhydride (Sigma-Aldrich Chemie, München, Germany) at 95 °C and pH 6.8 and washing twice in phosphate-buffered saline ([PBS], pH 7.4), slices were incubated with primary antibody (rabbit polyclonal anti-tyrosine hydroxylase, Abcam #ab112, diluted 1:100 in PBS) at 4 °C in a moisture chamber overnight. To remove unbound antibodies, slices were washed twice in PBS-T (containing 0.1% Tween20) and once in PBS followed by incubation with secondary antibody (anti-rabbit IgG FITC [Dianova, Hamburg, Germany, diluted 1:50 in PBS]) at 37 °C for 2 hours. Finally, slides were mounted with mounting medium (Vector Laboratories, Burlingame, USA, #H-1200) and stained with DAPI. Images were acquired as described above. Interstitial tyrosine hydroxylase–positive axons within 200 μm^2 areas were counted. To exclude nonspecific binding of the primary antibody, isotype controls were performed using a polyclonal rabbit IgG isotype control (Abcam #ab37415, diluted 1:100 in PBS).

ELISA

Concentrations of IS in plasma, urine, and hepatic tissue were determined by ELISA (Rat Indoxyl Sulfate ELISA Kit, MyBioSource, San Diego, CA) according to the manufacturer's protocol. Plasma IS was normalized to plasma total protein and urinary IS was normalized to the urinary creatinine concentration. Plasma concentrations of rat NT-proBNP (N-terminal pro-brain natriuretic peptide; MyBioSource, Catalog No:

MBS2509356) was determined by ELISA, following the manufacturer's protocol.

Determination of Renal Norepinephrine Content

Kidney tissue was minced thoroughly in TRIS-EDTA buffer (in mmol/L: 5.0 Tris(hydroxymethyl)aminomethane, 2.0 Na-EDTA, pH 7.4). After centrifugation, supernatants were used to analyze norepinephrine content by high-pressure liquid chromatography using Chromosystems plasma catecholamine Kit for HPLC (Chromosystems Instruments & Chemicals GmbH, Munich, Germany) following the manufacturer's protocol.

Liquid Chromatography–Mass Spectrometry/Mass Spectrometry

We measured liver indole concentrations using liquid chromatography tandem mass spectrometry. A detailed description is provided in Data S1. Indole was normalized to protein concentration in liver homogenates.

H9C2 Cell Culture

The immortalized rat cardiomyoblast cell line H9C2 was purchased from Sigma-Aldrich (Germany) and distributed to uncoated 6-well dishes. Each well was covered with 2 mL DMEM medium (Thermo Fisher Scientific) containing 10% fetal bovine serum and cells were incubated at 37 °C and 5% CO_2. After reaching a

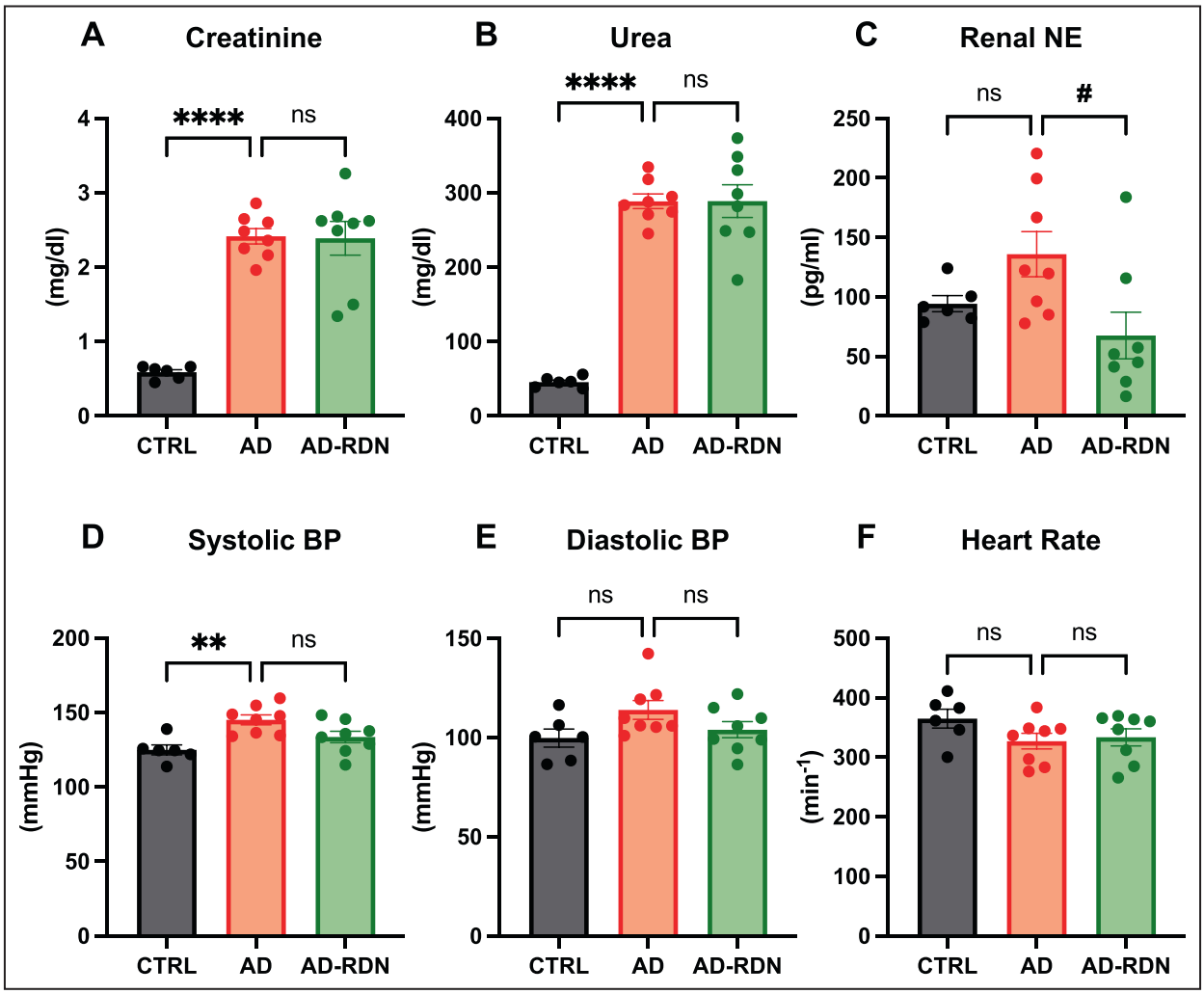

Figure 1. Kidney function, blood pressure, and renal norepinephrine.
CKD was confirmed in adenine-fed rats by elevated plasma concentration of creatinine and urea, which was unaltered by RDN (**A** and **B**). Analysis of renal norepinephrine (NE) content in kidneys demonstrated decreased NE level in AD-RDN (n=8) compared with AD (n=8) (**C**). Systolic BP as assessed by tail-cuff plethysmography or radiotelemetry and was increased in AD (n=8) compared with CTRL (n=6) (**D**). After RDN (n=8), systolic BP was not changed. Diastolic BP and heart rate were not significantly changed (**E** and **F**). Data are shown as mean±SEM. *P* value was determined using ANOVA with Tukey's test for multiple comparisons. AD indicates adenine-fed sham denervated group; AD-RDN, adenine-fed renal denervated group; BP, blood pressure; CKD, chronic kidney disease; CTRL, control group; NE, norepinephrine; ns, not significant; and RDN, renal denervation.

confluency of 80%, cells were covered with a hunger medium containing 0.1% fetal bovine serum. Stimulation experiments were performed with IS (Sigma-Aldrich) at concentrations of 10 μg/mL and 100 μg/mL over a period of 72 hours with daily stimulations. After 72 hours, cells were harvested and processed for FACS analysis as described below. For staining with hematoxylin and eosin: H9C2 cells were fixed in buffered 4% formaldehyde onto four six-well dishes per group and stained with hematoxylin and eosin (HE, Morphisto, Frankfurt a. M., Germany). For stimulation with conditioned media: H9C2 cells were cultured in 24 well-plates (Falcon; #353047) with 300 μL DMEM containing 10% heat-inactivated (30 minutes, 56 °C) rat serum (instead of FCS) derived from either CTRL, AD, or AD-RDN. After 72 hours, cells were stained with hematoxylin and eosin as described above. H9C2 cells treated with CTRL serum and 100 μg/mL IS served as internal positive control. Cell circumference and cell cross-sectional area was quantified from 400 cells/group using Nikon Instruments Software (NIS)-Elements (BR 3.2, Nikon instruments).

FACS

After removing cell culture medium, 500 μL trypsin was added to each well and cells were resuspended in 450 μL FACS buffer and 20 μL of 0.5 mol/L EDTA solution. The samples were then washed several times before the cells were finally resuspended in FACS buffer and 1% paraformaldehyde. Cell hypertrophy was estimated by the forward-scatter as a correlate of cell size via FACS analysis (BD FACSVerse).

Statistical Analysis

The data are presented as mean±SEM if not otherwise specified. Data were tested for normality using the Shapiro–Wilk test. Between-group differences were tested using univariate ANOVA with Tukey's post-hoc test for multiple comparisons if normality was assumed. If the assumption of normality was rejected, a nonparametric Kruskal–Wallis test was performed. All data were analyzed using GraphPad Prism 8.4.2 (GraphPad Software, Boston, MA). For comparison of 2 groups, an unpaired Student *t* test was used. A 2-sided *P* value of <0.05 was considered to be statistically significant. Additional permutational ANOVA in R using the one-way test function from the "coin" package were performed. Plain unadjusted *P* values are shown as well as adjusted *P* values for multiple comparison (ANOVA: Tukey's post-hoc test, Welch ANOVA: Dunnett's T3 test, Kruskal–Wallis: Dunn's test, permutational ANOVA: Bonferroni) are shown as Table S1 and Figure S1.

RESULTS

Kidney Function and Blood Pressure in CKD Remain Unchanged After RDN

CKD was confirmed in AD by elevated plasma concentrations of creatinine (2.42±0.1 versus 0.59±0.04 mg/dL, *P* <0.0001) and urea (289±9.9 versus 45.5±2.9 mg/dL, *P* <0.0001) compared with CTRL (Figure 1A and 1B). RDN had no effect on creatinine and urea concentration (2.39±0.23 mg/dL, *P*=0.99; 289±22 mg/dL, *P*=0.99) as

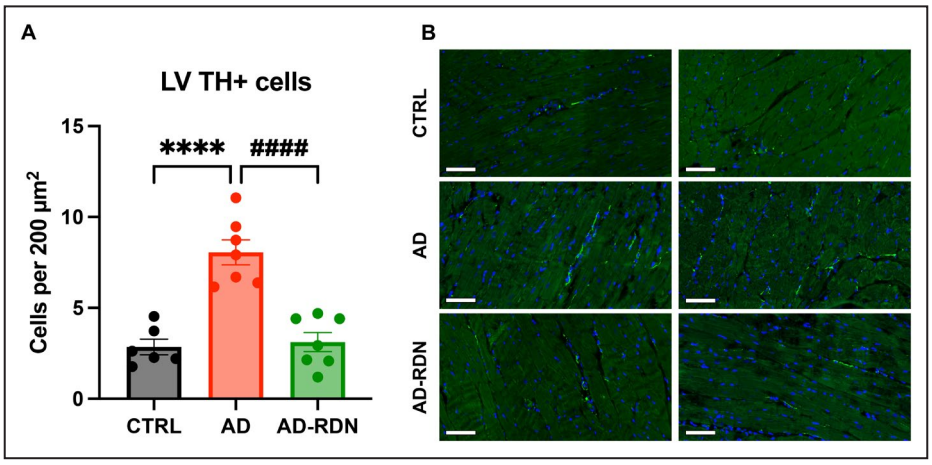

Figure 2. Increased left ventricular tyrosine hydroxylase expression in adenine-fed rats was reduced by RDN.
Quantification of left ventricular (LV) tyrosine hydroxylase–positive nerve fibers (**A**) and representative immunofluorescence staining of LV tyrosine hydroxylase in control (CTRL n=6), Adenine-fed rats (AD; n=7) and adenine-fed rats with renal denervation (AD-RDN; n=7) (**B**). Scale bar = 100 μm. Data are shown as mean±SEM. *P* value was determined using ANOVA with Tukey's test for multiple comparisons. AD indicates adenine-fed sham denervated group; AD-RDN, adenine-fed renal denervated group; CTRL, control group; and TH, tyrosine hydroxylase.

compared with AD. Effective RDN was demonstrated by reduced renal norepinephrine content (67.6±19.6 versus 136±19 pg/mL, P=0.025) (Figure 1C). Systolic blood pressure was increased in AD compared with CTRL (145.1±3.4 versus 124.9±3.3 mm Hg, P=0.0029). In AD-RDN, systolic blood pressure was not changed as compared with AD (133.6±3.9 mm Hg, P=0.069) (Figure 1D). Diastolic BP was not different among the groups (99.7±4.5 mm Hg in CTRL, 113.9±4.7 mm Hg in AD, P=0.10; 104±4.1 mm Hg in AD-RDN, P=0.25 versus AD) (Figure 1E). Also, heart rate was not significantly altered (364.9±15.8 min^{-1} in CTRL, 327±13.2 min^{-1} in AD, P=0.19; 265.8±14.3 min^{-1} in AD-RDN, P=0.94 versus AD) (Figure 1F).

RDN Decreases LV Sympathetic Innervation

In the LV, tyrosine hydroxylase–positive cells were significantly increased in AD as compared with CTRL (8.06±0.69 per 200 μm^2 versus 2.85±0.43 per 200 μm^2, P <0.0001), while RDN reduced LV tyrosine hydroxylase–positive cells (3.12±0.52 per 200 μm^2, P <0.0001) (Figure 2A and 2B).

RDN Reduces Myocardial Hypertrophy

LV myocardial hypertrophy was assessed by 3 different modalities. First, echocardiographic measurement revealed elevated thickness of the LV septal wall in AD (2.39±0.036 versus1.91±0.014 mm in CTRL, P <0.0001), which was reduced by RDN (1.97±0.054 mm, P <0.0001 versus AD) (Figure 3A). Figure 3B depicts representative echocardiograms in the parasternal long-axis view. LV diastolic function was estimated using E/A ratio. In AD, E/A was markedly increased (1.95±0.14 versus 1.06±0.03 in CTRL, P <0.0001) indicating elevated LV filling pressures. After RDN, E/A was decreased and comparable to CTRL (1.08±0.049, P <0.0001 versus AD) (Figure 3C). Mitral Doppler spectra are shown in Figure 3D. In line, plasma levels of N-terminal B-type natriuretic peptide were decreased following RDN (AD 6842 pg/mL versus AD-RDN 5584 pg/mL, P=0.016). Second, cardiac MRI demonstrated similar results with increased wall thickness of the anterior, posterior, and septal LV wall in AD (1.98±0.042 versus 1.68±0.053 mm in CTRL, P=0.0032; 1.79±0.017 versus 1.68±0.042 mm in CTRL, P=0.049; 1.93±0.043 versus 1.65±0.067 mm in CTRL, P=0.0073; respectively), which was reversed in AD-RDN (1.7±0.051 mm, P=0.009 versus AD; 1.66±0.03 mm, P=0.035 versus AD; 1.7±0.02 mm, P=0.033 versus AD; respectively) (Figure 4). In AD, peak filling rate (1642±95 versus 2383±290 µL/s in CTRL; P=0.06) end systolic volume (137±7 versus 158±6 µL in CTRL, P=0.25) and end diastolic volume (512±26 versus 563±19 µL in CTRL, P=0.86) were reduced compared with control. RDN attenuated impaired peak filling rate (1863±172 µL/s), end systolic volume (164±28 µL), and end diastolic volume

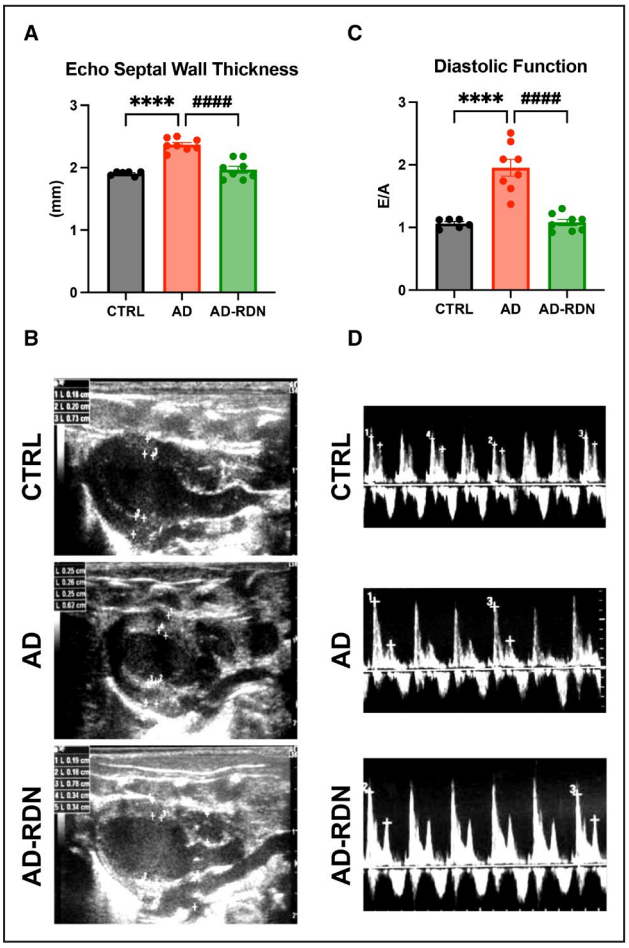

Figure 3. Increased septal wall thickness and impaired diastolic function was improved in AD-RDN.
Echocardiographic measurement of septal wall thickness (**A**). Adenine-fed rats AD (n=8) display increased wall thickness as compared with CTRL (n=6), which was normalized after RDN (n=8). Representative echocardiograms in parasternal long-axis (**B**). Diastolic function as assed by E/A ratio worsened in AD compared with CTRL and was significantly improved in AD-RDN (**C**). Representative PW Doppler spectra of transmitral velocity in early and late diastole (**D**). Data are shown as mean±SEM. P value was determined using ANOVA with Tukey's test for multiple comparisons. AD indicates adenine-fed sham denervated group; AD-RDN, adenine-fed renal denervated group; CTRL, control group; and RDN, renal denervation.

(553±97 µL/s). Ejection fraction was unchanged between groups (Table S2). Third, histological analysis of the cardiomyocyte cross-sectional area confirmed myocyte hypertrophy to contribute to LV wall thickening in AD (403±10.3 versus 331±9.1 μm^2 in CTRL, P=0.0008). In AD-RDN, myocyte size was decreased (349±12.4 μm^2, P=0.0057 versus AD) (Figure 5).

RDN Reduces Uremic Toxin IS in Liver and Plasma in CKD

Concentrations of IS in plasma and urine as well as hepatic tissue were measured. In plasma, IS

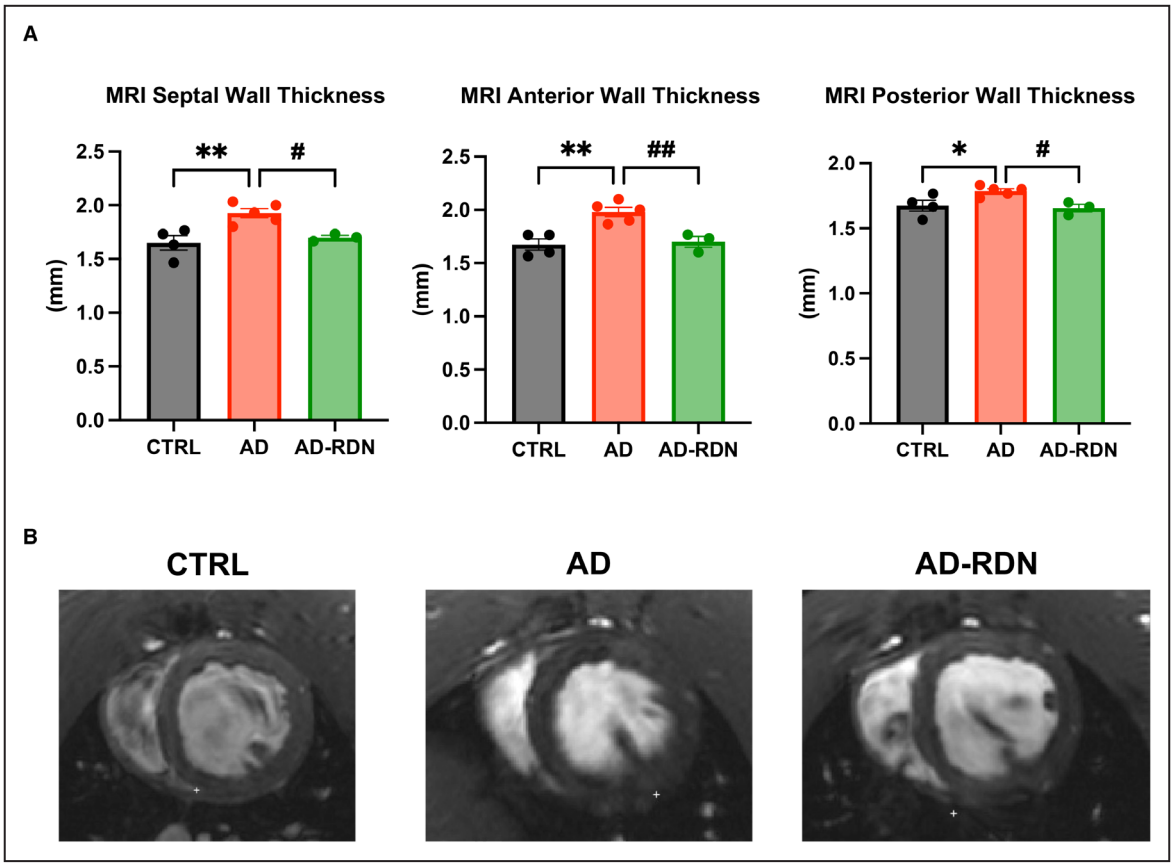

Figure 4. Adenine-induced left ventricular wall thickening was inhibited by RDN.
A, Quantification of the left ventricular (LV) anterior, posterior, and septal wall thickness demonstrated a significant increase in adenine-fed rats (AD, n=5) compared with control (CTRL, n=4), while wall thickening was prevented in AD-RDN (n=3). (**B**) Representative images in the short-axis view are shown in CTRL, AD, and AD-RDN. Data are shown as mean±SEM. *P* value was determined using ANOVA with Tukey's test for multiple comparisons. AD indicates adenine-fed sham denervated group; AD-RDN, adenine-fed renal denervated group; CTRL, control group; MRI, magnetic resonance imaging; and RDN, renal denervation.

concentration in AD was significantly elevated compared with CTRL (0.79±0.07 versus 0.2±0.12 μg/mg, *P*=0.0004) (Figure 6A). After RDN, plasma IS concentration was decreased (0.26±0.078 μg/mL, *P*=0.0006 versus AD). In urine, IS concentration was elevated both in AD and AD-RDN without significant difference between AD and AD-RDN (0.76±0.065 versus 0.79±0.058 μg/g, *P*=0.95 AD versus AD-RDN) (Figure 6A). IS concentration in hepatic tissue was increased only in AD (2.49±0.24 versus 1.63±0.28 μg/500 μg in CTRL, *P*=0.029) but not in AD-RDN (1.73±0.097 μg/500 μg, *P*=0.036 versus AD). Furthermore, there was a significant correlation between plasma IS concentrations and LV hypertrophy (r=0.779, *P* <0.0001) (Figure 6B). Liver indole concentrations were not significantly different among groups (Figure S2).

IS Induced Hypertrophy in H9C2 Cardiomyoblasts

In vitro experiments were conducted using H9C2 cells stimulated with IS. At 10 μg/mL, cell size as measured by forward scatter was only numerically increased (95.8±0.88 versus 94.8±1.04, *P*=0.74 versus Control), reaching statistical significance at 100 μg/mL (100.5±0.81, *P*=0.0015 versus Control) (Figure 6C). Histological analysis of H9C2 confirmed IS-induced hypertrophy, demonstrating a significantly increased cross-sectional area and cell diameter following treatment with 100 μg/mL IS (Figure 6D through 6F). Furthermore, we incubated H9C2 with conditioned medium containing serum of CTRL, AD, or AD-RDN rats. Cells incubated with medium derived from AD displayed significantly increased cell size (20 606±1443 μm^2 versus 15 460±1255 μm^2; *P*=0.029 versus CTRL), whereas incubation with medium derived from AD-RDN rats (15 893±1012 μm^2, *P*=0.031 versus AD) did not result in increased cell size as compared with CTRL (Figure 6H and 6I). The addition of IS to CTRL serum led to a similar effect on cellular hypertrophy as incubation with AD serum (15 460±1255 μm^2 versus 22 087±1971 μm^2, *P*=0.0016) (Figure 6G).

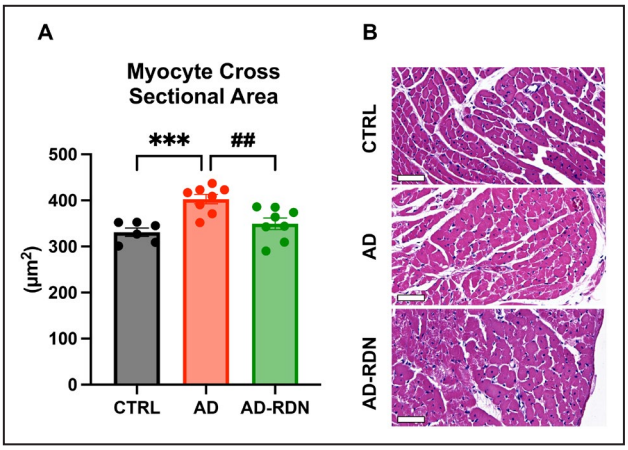

Figure 5. Adenine-induced left ventricular (LV) hypertrophy of cardiomyocytes was attenuated by RDN.
Quantification of cardiomyocyte cross-sectional area was increased in AD (n=8) compared with CTRL (n=6) and significantly decreased in AD-RDN (n=8) (**A**). Representative images of cardiomyocytes stained with hematoxylin and eosin (**B**). Scale bar=100 µm. Data are shown as mean±SEM. *P* value was determined using ANOVA with Tukey's test for multiple comparisons. AD indicates adenine-fed sham denervated group; AD-RDN, adenine-fed renal denervated group; CTRL, control group; and RDN, renal denervation.

DISCUSSION

In rats with CKD induced by adenine-enriched chow resulting in tubulo-interstitial nephropathy, RDN mitigates myocardial hypertrophy as assessed by echocardiography, MRI, and histological analysis. In rats with adenine-induced CKD, plasma concentrations of IS were elevated compared with CTRL and significantly decreased after RDN. Interestingly, urinary IS concentration was found to be similar in AD-RDN as compared with AD, whereas the hepatic concentration was significantly reduced after RDN. In H9C2 cells, stimulation with IS at concentrations observed in patients with CKD with end-stage renal disease induced cellular hypertrophy.

AD Model of CKD

In the AD model, a 0.25%-adenine-containing diet was used to induce tubulo-interstitial nephropathy.[14] Adenine is a purine base that converts to insoluble 2,8-dihydroxy-adenine. 2,8-Dihydroxy-adenine precipitates within renal tubules, causing the formation of crystals with consecutive obstruction. The pathophysiology as well as the resulting renal injury have been described in great detail elsewhere.[15] Adenine-induced CKD represents a suitable model for assessing cardiovascular complications concomitant with CKD, because rats develop uremic cardiomyopathy characterized by LV wall thickening, decreased LV cavity, and increased LV stiffness.[14]

Role of IS in Uremic Cardiomyopathy

Uremic cardiomyopathy is the result of several factors, among which uremic toxins play a key role.[16] LV hypertrophy represents a major issue inasmuch as it is a predictor of mortality.[17,18] Hitherto, approaches to treat LV hypertrophy mainly aim at controlling traditional risk factors, above all hypertension. Intestinal absorption of IS can be reduced by the oral charcoal adsorbent AST-120. In a rat model of CKD, rats fed with AST-120 showed less cardiac hypertrophy than controls.[19] However, in prospective human outcome trials, AST-120 failed to reduce cardiovascular and renal end points.[20,21] There is accumulating evidence that RDN reduces left ventricular hypertrophy in several models. In Dahl salt-sensitive rats, RDN led to a significant decrease in left ventricular mass.[22] Human trials enrolling patients with uncontrolled hypertension showed that RDN was able to reduce left ventricular mass independent of BP.[11,23]

Accumulation of uremic toxins in the circulation and tissues is associated with progression of kidney failure and its related comorbidities.[24] IS has been most frequently implicated as a contributor to renal disease progression and cardiovascular disease.[25]

We performed in vitro experiments using H9C2 rat embryonic cardiomyoblasts, a cell line that had been previously shown to mimic hypertrophic responses of neonatal cardiomyocytes,[26] to investigate the hypertrophic effect of IS. Our findings that IS induces hypertrophy in H9C2 are in line with previous experiments that demonstrated pro-hypertrophic effects of IS in vitro.[27] Forward scatter in FACS analysis provides a surrogate of cell size and was therefore used to determine myocyte hypertrophy as described before.[28] Additionally, treatment of H9C2 with conditioned medium (10% rat serum) derived from adenine-induced CKD-rats induced cell hypertrophy compared with control, whereas conditioned medium derived from adenine rats with RDN did not affect cell size. The higher amount of IS contained in the AD serum may have played a role here, because the addition of IS to CTRL serum yielded a similar effect as incubation with AD serum.

Metabolism of IS and Possible Mechanisms of RDN-Dependent Regulation

IS originates from indole, which is produced by intestinal bacteria metabolizing dietary tryptophan.[29] After absorption, indole reaches the liver, where it enters phase I and II of bio-transformation, ultimately being released as IS into the systemic circulation.[30,31] Since IS is highly bound to albumin,[32] it is excreted by the kidneys mainly through active tubular secretion via organic anion transporters.[33] Hence, IS cannot be

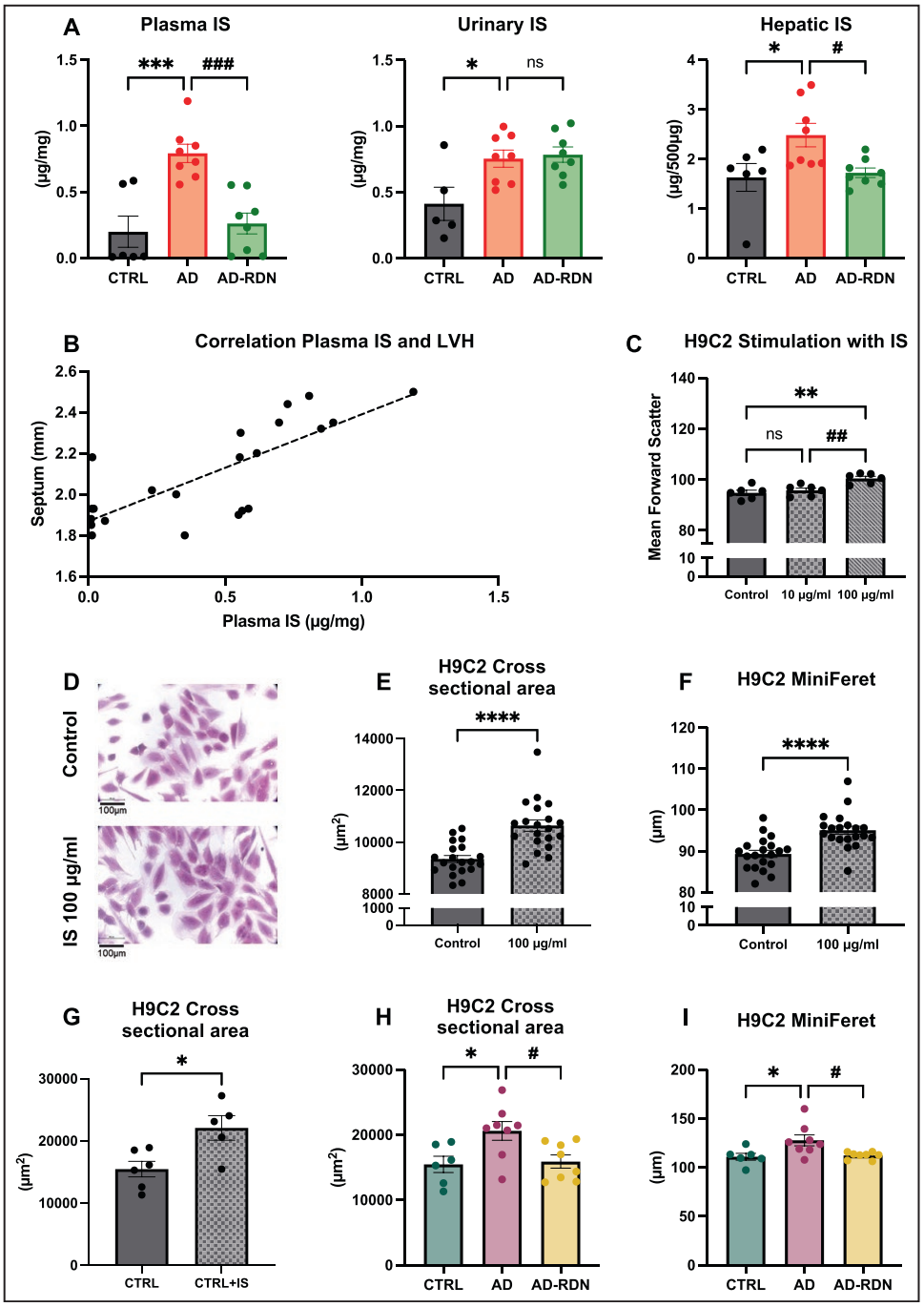

Figure 6. Indoxyl sulfate (IS) is associated with hypertrophy.
Plasma IS concentration was significantly increased in AD (n=8) but not in AD-RDN (n=8) (**A**). Urine IS excretion did not differ between AD (n=8) and AD-RDN (n=8), whereas hepatic IS was significantly decreased in AD-RDN. Plasma IS concentration correlated with septal wall thickness (n=22) (**B**). H9C2 stimulation with IS led to a numerical increase in cell size at 10 µg/mL, reaching statistical significance at 100 µg/mL (n=6 each) (**C**). Representative images of H9C2 cells stimulated with IS (100 µg/mL) and stained with hematoxylin and eosin (**D**). Cross-sectional area and MiniFeret (smallest diameter) of H9C2 significantly increases after treatment with 100 µg/mL IS compared with control (CTRL) (**E** and **F**). Incubation with sera derived from AD produced cellular hypertrophy as compared with CTRL and AD-RDN (**H** and **I**). Addition of IS to CTRL serum led to a similar hypertrophic effect (**G**). Each data point represents the mean value of 20 H9C2 cells. Altogether, 400 cells per group were analyzed. Data are shown as mean±SEM. *P* value was determined using ANOVA and Tukey's multiple comparisons test for comparison of 3 groups. An unpaired t test was used for comparison of 2 groups. AD indicates adenine-fed sham denervated group; AD-RDN, adenine-fed renal denervated group; CTRL, control group; IS, indoxyl sulfate; LVH, left ventricular hypertrophy; and ns, not significant.

effectively removed by hemodialysis and its toxicity remains a major issue in patients with end-stage renal disease.[3] Previous in vitro studies have suggested that IS has pro-hypertrophic effects on both neonatal and adult cardiomyocytes.[6,27] Furthermore, there is in vivo evidence that IS induces cardiac hypertrophy in rats with subtotal nephrectomy,[7] adenine-induced CKD,[34] and rats with IS administration.[35] Prospective clinical trials support the hypothesis that IS even has prognostic significance in patients with CKD and concomitant CVD.[36–38] Against this background, our results appear particularly relevant. We found that plasma IS was elevated in AD rats compared with CTRL, which was markedly reduced after RDN. To ascertain whether this effect is due to an increased renal excretion or a decreased IS production, we measured both urinary and hepatic concentrations of IS. Interestingly, urinary excretion of IS did not differ between AD and AD-RDN, albeit elevated as compared with CTRL. However, hepatic concentration of IS was significantly increased in AD and reduced after RDN. Therefore, we suggest that RDN reduces the hepatic production of IS, thus resulting in decreased IS plasma levels.

One possible mechanism leading to decreased hepatic IS production would be the altered intestinal absorption of indole. Patients with CKD exhibit certain intestinal pathologies, in particular intestinal epithelial barrier dysfunction and dysbiosis.[39,40] As a consequence, malfunction of the intestinal barrier renders these patients vulnerable to absorption of small molecules leading to systemic inflammation and uremic toxicity. A major constituent of this barrier are tight junction proteins connecting the epithelial enterocytes to regulate paracellular diffusion. In uremic 5/6 nephrectomized rats, the expression of intestinal tight junction proteins is down-regulated.[41] Elevated urea and ammonium concentrations have been proposed as possible mechanisms causing the disruption of the intestinal barrier.[42] In addition to the increased intestinal permeability in CKD, dysbiosis further aggravates the production of uremic toxins. In CKD, the microbiome is altered in a fashion that is characterized by the expansion of tryptophanase-expressing families such as *Clostridiaceae* and *Enterobacteriaceae*, thus contributing to the production of indole.[43] From a general perspective, uremic toxicity is not only a result of insufficient renal excretory function, but also from an increased intestinal permeability and increased synthesis of precursor molecules.[44] This leads us to the second possible mechanism for the observed reduction in hepatic IS production, namely, a liver-specific intrinsic change in the indole procession, through for example an altered activity of the enzymes involved in the process. Because RDN is known to reduce efferent sympathetic outflow to peripheral organs, this raises the interesting question of whether RDN is able to modify the hepatic and enteric nervous system as well. CKD is associated with disruption of the intestinal barrier structure,[44] altered reactivity, and cholinergic signaling of the enteric nervous system, effecting absorptive and secretory processes,[45] events that play a major role in the pathogenesis of uremic toxicity. It has been shown that RDN decreased renal and intestinal sympathetic nerve activity in rats with myocardial infarction. This was associated with improved intestinal structure, permeability, reduced plasma lipopolysaccharide and ameliorated the gut microbial dysbiosis.[46] In rats with heart failure, RDN improved intestinal barrier function and mediated beneficial effects on the gut microbiota.[47] Therefore, it is conceivable that RDN may also improve intestinal injury in CKD effecting gut-derived uremic toxicity.

Limitations

Our study has some potential limitations. First, the number of animals is relatively low and may decrease statistical power. Second, the animal model of adenine-induced CKD does not imitate human CKD in every aspect. Although CKD in humans originates predominantly from glomerular injury secondary to hypertension and diabetes, adenine-induced nephropathy leads primarily to tubular injury due to precipitation of adenine crystals with concomitant renal interstitial inflammation and injury. Third, despite IS being quantitatively the most dominant uremic toxin that cannot be dialyzed, there are several other uremic toxins, which might influence uremic cardiomyopathy and that could not be addressed in this study. Fourth, we did not assess liver and intestinal sympathetic innervation nor liver indole detoxification steps or gut permeability, which is beyond the scope of this study.

CONCLUSIONS

In a rat model of CKD, RDN reduced plasma IS and mitigated the development of left ventricular hypertrophy independent of blood pressure. It is conceivable that hepatic IS production is decreased by RDN.

ARTICLE INFORMATION

Received September 10, 2024; accepted May 21, 2025.

Affiliations

Klinik für Innere Medizin III (P.M., M. Tokcan, M. Therre, F.M., M.B.), Klinik für Innere Medizin IV (S-R.S., S.J.S.) and Klinik für Diagnostische und Interventionelle Radiologie, Universität des Saarlandes, Homburg, Germany (M.H., A.M.), Institut für Medizinische Biometrie, Epidemiologie und Medizinische Informatik, Saarland University, Homburg/Saar, Germany (S.W.); Institute of Experimental and Clinical Pharmacology and Toxicology, Saarland University, Homburg, Germany (L.W.); Aachen-Maastricht Institute for CardioRenal Disease (AMICARE) (E.P.v.d.V.), Institute for Molecular Cardiovascular Research (IMCAR) (E.P.v.d.V., H.N., J.W.) and Interdisciplinary Center for Clinical Research (IZKF), RWTH Aachen University, Aachen, Germany (F.K., E.P.v.d.V.)Institute for Cardiovascular Prevention (IPEK),

Ludwig-Maximilians-University Munich, Munich, Germany (E.P.v.d.V.); Department of Internal Medicine I, University Hospital Aachen, RWTH Aachen University, Aachen, Germany (M.R.); Department of Cardiology, University Heart Center, University Hospital Basel, Basel, Switzerland (F.M.); and Cardiovascular Research Institute Basel (CRIB), University Heart Center, University Hospital Basel, Basel, Switzerland (F.M.).

Acknowledgments

We thank Laura Frisch and Simone Jäger for excellent technical assistance.

Sources of Funding

This work was supported by the German Research Foundation (DFG) (TRR219-M02; -S02, Project-ID 322900939) and by a grant from the Interdisciplinary Center for Clinical Research, Faculty of Medicine, RWTH Aachen University, by the German Research Foundation (DFG) (SFB TRR219-M07), and by the Corona Foundation (S199/10084/2021) to E.P.C.van der Vorst. F. Kahles was funded by the German Research Foundation (DFG, German Research Foundation, 520275106, Emmy Noether Research Group, SFB TRR 219-322 900 939-M-07).

Disclosures

F. Mahfoud has received scientific support and speaker honoraria from Bayer, Boehringer Ingelheim, Medtronic, and ReCor Medical. M. Böhm reports personal fees from Abbott, Amgen, AstraZeneca, Bayer, Boehringer Ingelheim, Cytokinetics, Medtronic, Novartis, Servier, and Vifor. The other authors do not declare any conflict of interest.

Supplemental Material

Data S1
Tables S1–S2
Figures S1–S2
Reference 48

REFERENCES

1. Jankowski J, Floege J, Fliser D, Böhm M, Marx N. Cardiovascular disease in chronic kidney disease. *Circulation*. 2021;143:1157–1172. doi: 10.1161/CIRCULATIONAHA.120.050686
2. Weiner DE, Tighiouart H, Elsayed EF, Griffith JL, Salem DN, Levey AS, Sarnak MJ. The Framingham predictive instrument in chronic kidney disease. *J Am Coll Cardiol*. 2007;50:217–224. doi: 10.1016/j.jacc.2007.03.037
3. Lekawanvijit S. Cardiotoxicity of uremic toxins: a driver of cardiorenal syndrome. *Toxins*. 2018;10:352. doi: 10.3390/toxins10090352
4. McCullough PA, Kellum JA, Haase M, Müller C, Damman K, Murray PT, Cruz D, House AA, Schmidt-Ott KM, Vescovo G, et al. Pathophysiology of the cardiorenal syndromes: executive summary from the eleventh consensus conference of the acute dialysis quality initiative (ADQI). *Contrib Nephrol*. 2013;182:82–98. doi: 10.1159/000349966
5. Vanholder R, Schepers E, Pletinck A, Nagler EV, Glorieux G. The uremic toxicity of indoxyl sulfate and *P*-Cresyl sulfate: a systematic review. *J Am Soc Nephrol*. 2014;25:1897–1907. doi: 10.1681/ASN.2013101062
6. Lekawanvijit S, Adrahtas A, Kelly DJ, Kompa AR, Wang BH, Krum H. Does indoxyl sulfate, a uraemic toxin, have direct effects on cardiac fibroblasts and myocytes? *Eur Heart J*. 2010;31:1771–1779. doi: 10.1093/eurheartj/ehp574
7. Lekawanvijit S, Kompa AR, Manabe M, Wang BH, Langham RG, Nishijima F, Kelly DJ, Krum H. Chronic kidney disease-induced cardiac fibrosis is ameliorated by reducing circulating levels of a non-Dialysable uremic toxin, indoxyl sulfate. *PLoS One*. 2012;7:e41281. doi: 10.1371/journal.pone.0041281
8. Kaur J, Young BE, Fadel PJ. Sympathetic overactivity in chronic kidney disease: consequences and mechanisms. *Int J Mol Sci*. 2017;18:1682. doi: 10.3390/ijms18081682
9. Zoccali C, Mallamaci F, Parlongo S, Cutrupi S, Benedetto FA, Tripepi G, Bonanno G, Rapisarda F, Fatuzzo P, Seminara G, et al. Plasma norepinephrine predicts survival and incident cardiovascular events in patients with end-stage renal disease. *Circulation*. 2002;105:1354–1359. doi: 10.1161/hc1102.105261
10. Biffi A, Dell'Oro R, Quarti-Trevano F, Cuspidi C, Corrao G, Mancia G, Grassi G. Effects of renal denervation on sympathetic nerve traffic and correlates in drug-resistant and uncontrolled hypertension: a systematic review and meta-analysis. *Hypertension*. 2023;80:659–667. doi: 10.1161/HYPERTENSIONAHA.122.20503
11. Mahfoud F, Urban D, Teller D, Linz D, Stawowy P, Hassel J-H, Fries P, Dreysse S, Wellnhofer E, Schneider G, et al. Effect of renal denervation on left ventricular mass and function in patients with resistant hypertension: data from a multi-centre cardiovascular magnetic resonance imaging trial. *Eur Heart J*. 2014;35:2224–2231. doi: 10.1093/eurheartj/ehu093
12. Linz B, Hohl M, Lang L, Wong DWL, Nickel AG, De La Torre C, Sticht C, Wirth K, Boor P, Maack C, et al. Repeated exposure to transient obstructive sleep apnea–related conditions causes an atrial fibrillation substrate in a chronic rat model. *Heart Rhythm*. 2021;18:455–464. doi: 10.1016/j.hrthm.2020.10.011
13. Linz D, Hohl M, Schütze J, Mahfoud F, Speer T, Linz B, Hübschle T, Juretschke H-P, Dechend R, Geisel J, et al. Progression of kidney injury and cardiac remodeling in obese spontaneously hypertensive rats: the role of renal sympathetic innervation. *Am J Hypertens*. 2014;28:256–265. doi: 10.1093/ajh/hpu123
14. Diwan V, Brown L, Gobe GC. Adenine-induced chronic kidney disease in rats. *Nephrology*. 2018;23:5–11. doi: 10.1111/nep.13180
15. Klinkhammer BM, Djudjaj S, Kunter U, Palsson R, Edvardsson VO, Wiech T, Thorsteinsdottir M, Hardarson S, Foresto-Neto O, Mulay SR, et al. Cellular and molecular mechanisms of kidney injury in 2,8-dihydroxyadenine nephropathy. *J Am Soc Nephrol*. 2020;31:799–816. doi: 10.1681/ASN.2019080827
16. de Albuquerque Suassuna PG, Sanders-Pinheiro H, de Paula RB. Uremic cardiomyopathy: a new piece in the chronic kidney disease-mineral and bone disorder puzzle. *Front Med*. 2018;5:5. doi: 10.3389/fmed.2018.00206
17. Parfrey PS, Harriett JD, Griffiths SM, Taylor R, Harnett JD, King A, Barre PE. The clinical course of left ventricular hypertrophy in dialysis patients. *Nephron*. 1990;55:114–120. doi: 10.1159/000185937
18. Zoccali C, Benedetto FA, Mallamaci F, Tripepi G, Giacone G, Stancanelli B, Cataliotti A, Malatino LS. Left ventricular mass monitoring in the follow-up of dialysis patients: prognostic value of left ventricular hypertrophy progression. *Kidney Int*. 2004;65:1492–1498. doi: 10.1111/j.1523-1755.2004.00530.x
19. Fujii H, Nishijima F, Goto S, Sugano M, Yamato H, Kitazawa R, Kitazawa S, Fukagawa M. Oral charcoal adsorbent (AST-120) prevents progression of cardiac damage in chronic kidney disease through suppression of oxidative stress. *Nephrol Dial Transplant*. 2009;24:2089–2095. doi: 10.1093/ndt/gfp007
20. Schulman G, Berl T, Beck GJ, Remuzzi G, Ritz E, Arita K, Kato A, Shimizu M. Randomized placebo-controlled EPPIC trials of AST-120 in CKD. *J Am Soc Nephrol*. 2015;26:1732–1746. doi: 10.1681/ASN.2014010042
21. Cha R-h, Kang SW, Park CW, Cha DR, Na KY, Kim SG, Yoon SA, Han SY, Chang JH, Park SK, et al. A randomized, controlled trial of Oral intestinal sorbent AST-120 on renal function deterioration in patients with advanced renal dysfunction. *Clin J Am Soc Nephrol*. 2016;11:559–567. doi: 10.2215/CJN.12011214
22. Watanabe H, Iwanaga Y, Miyaji Y, Yamamoto H, Miyazaki S. Renal denervation mitigates cardiac remodeling and renal damage in dahl rats: a comparison with β-receptor blockade. *Hypertens Res*. 2016;39:217–226. doi: 10.1038/hr.2015.133
23. Schirmer SH, Sayed MMYA, Reil J-C, Ukena C, Linz D, Kindermann M, Laufs U, Mahfoud F, Böhm M. Improvements in left ventricular hypertrophy and diastolic function following renal denervation: effects beyond blood pressure and heart rate reduction. *J Am Coll Cardiol*. 2014;63:1916–1923. doi: 10.1016/j.jacc.2013.10.073
24. Lim YJ, Sidor NA, Tonial NC, Che A, Urquhart BL. Uremic toxins in the progression of chronic kidney disease and cardiovascular disease: mechanisms and therapeutic targets. *Toxins*. 2021;13:142. doi: 10.3390/toxins13020142
25. Leong SC, Sirich TL. Indoxyl sulfate-review of toxicity and therapeutic strategies. *Toxins*. 2016;8:358. doi: 10.3390/toxins8120358
26. Watkins SJ, Borthwick GM, Arthur HM. The H9C2 cell line and primary neonatal cardiomyocyte cells show similar hypertrophic responses in vitro. *In Vitro Cell Dev Biol - Anim*. 2011;47:125–131. doi: 10.1007/s11626-010-9368-1
27. Yang K, Xu X, Nie L, Xiao T, Guan X, He T, Yu Y, Liu L, Huang Y, Zhang J, et al. Indoxyl sulfate induces oxidative stress and hypertrophy in cardiomyocytes by inhibiting the AMPK/UCP2 signaling pathway. *Toxicol Lett*. 2015;234:110–119. doi: 10.1016/j.toxlet.2015.01.021

28. Brunt KR, Tsuji MR, Lai JH, Kinobe RT, Durante W, Claycomb WC, Ward CA, Melo LG. Heme Oxygenase-1 inhibits pro-oxidant induced hypertrophy in HL-1 cardiomyocytes. *Exp Biol Med*. 2009;234:582–594. doi: 10.3181/0810-RM-312
29. Neves AL, Chilloux J, Sarafian MH, Rahim MBA, Boulangé CL, Dumas M-E. The microbiome and its pharmacological targets: therapeutic avenues in cardiometabolic diseases. *Curr Opin Pharmacol*. 2015;25:36–44. doi: 10.1016/j.coph.2015.09.013
30. Banoglu E, Jha GG, King RS. Hepatic microsomal metabolism of indole to indoxyl, a precursor of indoxyl sulfate. *Eur J Drug Metab Pharmacokinet*. 2001;26:235–240. doi: 10.1007/BF03226377
31. Banoglu E, King RS. Sulfation of indoxyl by human and rat aryl (phenol) sulfotransferases to form indoxyl sulfate. *Eur J Drug Metab Pharmacokinet*. 2002;27:135–140. doi: 10.1007/BF03190428
32. Viaene L, Annaert P, de Loor H, Poesen R, Evenepoel P, Meijers B. Albumin is the main plasma binding protein for indoxyl sulfate and P-cresyl sulfate. *Biopharm Drug Dispos*. 2013;34:165–175. doi: 10.1002/bdd.1834
33. Deguchi T, Kusuhara H, Takadate A, Endou H, Otagiri M, Sugiyama Y. Characterization of uremic toxin transport by organic anion transporters in the kidney. *Kidney Int*. 2004;65:162–174. doi: 10.1111/j.1523-1755.2004.00354.x
34. Kashioulis P, Lundgren J, Shubbar E, Nguy L, Saeed A, Guron CW, Guron G. Adenine-induced chronic renal failure in rats: a model of chronic Renocardiac syndrome with left ventricular diastolic dysfunction but preserved ejection fraction. *Kidney Blood Press Res*. 2018;43:1053–1064. doi: 10.1159/000491056
35. Yisireyili M, Shimizu H, Saito S, Enomoto A, Nishijima F, Niwa T. Indoxyl sulfate promotes cardiac fibrosis with enhanced oxidative stress in hypertensive rats. *Life Sci*. 2013;92:1180–1185. doi: 10.1016/j.lfs.2013.05.008
36. Yoshikawa D, Ishii H, Suzuki S, Takeshita K, Kumagai S, Hayashi M, Niwa T, Izawa H, Murohara T. Plasma indoxyl sulfate and estimated glomerular filtration rate—association with long-term clinical outcome in patients with coronary artery disease. *Circ J*. 2014;78:2477–2482. doi: 10.1253/circj.CJ-14-0401
37. Watanabe I, Tatebe J, Fujii T, Noike R, Saito D, Koike H, Yabe T, Okubo R, Nakanishi R, Amano H, et al. Prognostic utility of indoxyl sulfate for patients with acute coronary syndrome. *J Atheroscler Thromb*. 2019;26:64–71. doi: 10.5551/jat.44149
38. Watanabe I, Tatebe J, Fujii T, Noike R, Saito D, Koike H, Yabe T, Okubo R, Nakanishi R, Amano H, et al. Prognostic significance of serum indoxyl sulfate and albumin for patients with cardiovascular disease. *Int Heart J*. 2019;60:129–135. doi: 10.1536/ihj.18-116
39. Vaziri ND, Zhao Y-Y, Pahl MV. Altered intestinal microbial flora and impaired epithelial barrier structure and function in CKD: the nature, mechanisms, consequences and potential treatment. *Nephrol Dial Transplant*. 2015;31:737–746. doi: 10.1093/ndt/gfv095
40. Andersen K, Kesper MS, Marschner JA, Konrad L, Ryu M, Kumar VRS, Kulkarni OP, Mulay SR, Romoli S, Demleitner J, et al. Intestinal dysbiosis, barrier dysfunction, and bacterial translocation account for CKD–related systemic inflammation. *J Am Soc Nephrol*. 2017;28:76–83. doi: 10.1681/asn.2015111285
41. Vaziri ND, Yuan J, Rahimi A, Ni Z, Said H, Subramanian VS. Disintegration of colonic epithelial tight junction in uremia: a likely cause of CKD-associated inflammation. *Nephrol Dial Transplant*. 2011;27:2686–2693. doi: 10.1093/ndt/gfr624
42. Vaziri ND, Yuan J, Norris K. Role of urea in intestinal barrier dysfunction and disruption of epithelial tight junction in chronic kidney disease. *Am J Nephrol*. 2013;37:1–6. doi: 10.1159/000345969
43. Wong J, Piceno YM, DeSantis TZ, Pahl M, Andersen GL, Vaziri ND. Expansion of urease- and uricase-containing, indole- and *P*-cresol-forming and contraction of short-chain fatty acid-producing intestinal microbiota in ESRD. *Am J Nephrol*. 2014;39:230–237. doi: 10.1159/000360010
44. Vaziri ND. CKD impairs barrier function and alters microbial flora of the intestine: a major link to inflammation and uremic toxicity. *Curr Opin Nephrol Hypertens*. 2012;21:587–592. doi: 10.1097/MNH.0b013e328358c8d5
45. Almeida PP, Thomasi BBM, Menezes ÁC, Da Cruz BO, Costa NS, Brito ML, Pereira ADA, Castañon CR, Degani VAN, Magliano DAC, et al. 5/6 nephrectomy affects enteric glial cells and promotes impaired antioxidant defense in the colonic neuromuscular layer. *Life Sci*. 2022;298:120494. doi: 10.1016/j.lfs.2022.120494
46. Huo J-Y, Jiang W-Y, Lyu Y-T, Zhu L, Liu H-H, Chen Y-Y, Chen M, Geng J, Jiang Z-X, Shan Q-J. Renal denervation attenuates neuroinflammation in the brain by regulating gut-brain Axis in rats with myocardial infarction. *Front Cardiovasc Med*. 2021;8:650140. doi: 10.3389/fcvm.2021.650140
47. Guo Z, Chen F, Chen Y, Liu C, Li S, Chen P. Inhibiting intestinal Krüppel-like factor 5 impairs the beneficial role of renal denervation in gut microbiota in rats with heart failure. *Microbiol Spectr*. 2022;10:e02183-22. doi: 10.1128/spectrum.02183-22
48. Joshi V, Chhonker YS, Soni D, Cunningham KC, Samuelson DR, Murry DJ. A selective and sensitive LC-MS/MS method for quantitation of indole in mouse serum and tissues. *Metabolites*. 2022;12:716. doi: 10.3390/metabo12080716